State-Resolved Studies of Collisional Quenching of Highly Vibrationally Excited Pyrazine by Water: The Case of the Missing V → RT Supercollision Channel

Margaret Fraelich, Michael S. Elioff, and Amy S. Mullin*

Department of Chemistry, Metcalf Center for Science and Engineering, Boston University, Boston, Massachusetts 02215

Received: June 12, 1998; In Final Form: August 27, 1998

The quenching of highly vibrationally excited pyrazine through collisions with H_2O at 300 K in a low-pressure environment was investigated using high-resolution transient absorption spectroscopy of water at $\lambda \approx 2.7$ μm. Highly vibrationally excited pyrazine with $E_{vib} = 37\,900$ cm^{-1} was prepared by absorption of 266 nm light to the electronically excited S_2 state, followed by rapid radiationless decay to the ground electronic state. Collisions between highly excited pyrazine and water that result in rotational and translational excitation of the vibrationless ground state of H_2O (000) were investigated by measuring the state-resolved appearance of individual rotational states of H_2O (000). Transient absorption measurements have been made on numerous rotational states to determine the nascent distribution of rotational energy gain in water. Doppler-broadened transient absorption line shapes were collected for a number of rotational levels in the (000) state in order to measure velocity distributions of the scattered water molecules. The nascent distribution of water rotational states with $E_{rot} > 1000$ cm^{-1} is well described by $T_{rot} = 920$ K, and the velocity distributions correspond to $T_{trans} \approx 560$ K, independent of the rotational state. Rate constants for energy gain into individual quantum states of H_2O (000) from collisions with hot pyrazine provide a measure of the high-energy part of the energy-transfer probability distribution function. The quenching of hot pyrazine through collisions with water displays a significant reduction in the bath translational energy gain when compared to earlier studies on the quenching of hot pyrazine ($E_{vib} = 37\,900$ cm^{-1}) by CO_2 {Wall, M. C.; Mullin, A. S. *J. Chem. Phys.* **1998**, *108*, 9658}. A comparison of the two systems provides insights into the molecular properties that influence the relaxation of highly vibrationally excited molecules.

Introduction

Highly vibrationally excited molecules play a significant role in a diverse range of activated chemical and physical processes, and understanding the collisional deactivation of these molecules is critical for developing models of molecular behavior at high energies.[1−4] Water is an especially important species in collisional quenching processes due to its ubiquity in combustion, atmospheric environments, and acoustic transport phenomena. Therefore, it is highly desirable to understand in detail the mechanisms and probabilities for collisional relaxation of highly excited molecules in the presence of water. Recently, state-resolved studies of collisional energy transfer from highly excited donors have revealed that, at least for energy-accepting molecules such as CO_2 and N_2O, substantial energy gain into rotation and translation of the surrounding bath molecules plays a very important role in the overall relaxation. There is evidence that rotational and translational excitation of the bath is primarily responsible for the high-energy tail of the energy-transfer probability distribution function, $P(E,E')$, for a number of donor/acceptor pairs. The goal of the present experiments is to determine whether a similar energy-transfer process is operative when water is the energy-accepting bath molecule.

Water is of special interest as a bath because previous studies have indicated that its behavior is quite unusual when compared to nonpolar quenchers such as CO_2 or O_2. Water demonstrates an enhanced ability to quench low levels of vibrational excitation in small molecules relative to other energy acceptors.[5] For instance, the collisional relaxation of CO_2 (01^10) at 300 K occurs 100 times more readily in the presence of H_2O (000) than with CO_2 (00^00) as a collision partner.[6] In another example, the quenching of O_2 ($v = 1$) by H_2O (000) is 10^4 times faster than relaxation through collisions with O_2 ($v = 0$), despite an unfavorable energy gap.[7] As a quencher of highly vibrationally excited molecules, water also demonstrates outstanding efficiencies. This is apparent in results from UV absorption,[8−10] IR, fluorescence,[11−13] and thermal lensing[14] experiments that measure energy loss from highly excited molecules in the presence of different quenching species. These techniques have been very successful in establishing the overall quenching effectiveness of a wide range of energy-accepting molecules. Such studies have shown that the average energy transfer per collision, $\langle\langle \Delta E \rangle\rangle$, generally increases with the increasing complexity of the bath gas and that polar polyatomic bath molecules are more efficient quenchers than nonpolar molecules of comparable complexity. This trend is evident when the quenching efficiencies for CO_2 and H_2O are compared for several high-energy donors. For example, benzene with $E_{vib} = 24\,000$ cm^{-1} transfers, on average, 208 cm^{-1} in collisions with CO_2 and as much as 373 cm^{-1} when H_2O is the collision partner.[11] Similarly, collisions of CO_2 and azulene with 24 000 cm^{-1} of internal energy result in $\langle\langle \Delta E \rangle\rangle = 360$ cm^{-1} while for collisions of H_2O with excited azulene, $\langle\langle \Delta E \rangle\rangle = 480$ cm^{-1}.[9] Water has also been reported to be a particularly efficient quencher of triplet pyrazine containing 5000 cm^{-1} of vibrational energy, with $\langle\langle \Delta E \rangle\rangle = 655$ cm^{-1} per collision as compared to only $\langle\langle \Delta E \rangle\rangle = 217$ cm^{-1} for a CO_2 bath.[15]

10.1021/jp982608o CCC: $15.00
Published on Web 11/03/1998

Recently, a microscopic picture of the collisional relaxation of highly excited molecules has emerged through state-resolved transient IR absorption studies of the energy gain in bath molecules performed initially by Flynn and co-workers[16−21] and subsequently by Mullin and co-workers.[22−24] By focusing on energy gain in the bath molecules, specific energy-transfer pathways can be identified and characterized. This approach has already provided important insights into the microscopic mechanisms of energy transfer from highly excited molecules and is now beginning to reveal molecular details of energy-dependent energy transfer.[24,25] Distinct state-specific relaxation pathways have been identified in these studies and appear to be common to the bath species that have been studied. To date, only two bath molecules, CO_2 and N_2O, have been studied with this technique and it is unknown whether the observed mechanisms are common to all types of energy-accepting molecules. In light of water's environmental importance and its relatively large $\langle\langle \Delta E \rangle\rangle$ values, it is interesting to consider how various energy-transfer mechanisms contribute to the enhanced quenching efficiency of water.

Transient high-resolution IR laser probing of energy gain in bath molecules following collisions with highly excited donors reveals an enormous amount about the collisional relaxation of highly excited molecules. Among the key pieces of information from this technique are the nascent population distributions of the scattered bath molecules, the partitioning of the exchanged energy into the bath degrees of freedom, and the state-specific rate constants for the various relaxation pathways. Taken together, these data help identify the predominant and secondary relaxation mechanisms that lead back to thermal equilibrium. When energy-dependent measurements are made, insight into the relative importance of competing pathways for various donor energies can be gained as well. Transient IR absorption studies on CO_2 have highlighted the predominance of energy transfer involving large rotational and translational (V → RT) energy gain in CO_2 (00^00) following collisions with a number of highly vibrationally excited donors. These studies include the relaxation of pyrazine (E_{vib} = 40 680 cm^{-1}),[17,18] pyrazine (E_{vib} = 37 900 cm^{-1}),[23] hexafluorobenzene (E_{vib} = 40 680 cm^{-1}),[20] and pyridine (E_{vib} = 37 900 cm^{-1})[22] as well as energy-dependent studies on pyrazine (E_{vib} = 30000−41000 cm^{-1}).[24,25] The V → RT energy-transfer pathway can result in a substantial loss of donor vibrational energy (as much as 8000 cm^{-1} in a single collision for the pyrazine/CO_2 system) that generates highly excited bath rotations and translation. In some cases, for example, collisions between highly excited pyrazine (E_{vib} = 37 900 cm^{-1}) and CO_2, this can result in a subset of CO_2 (00^00) molecules that are rotationally hot ($T_{rot} \approx$ 1200 K for J = 56−84) as well as translationally excited ($T_{trans} \approx$ 1000−4000 K). Such collisions have been identified as "supercollisions", whereby large amounts of energy are lost from the donor molecule in a single collision. For the pyrazine/CO_2 system, this type of large-magnitude V → RT energy transfer is the source of the high-energy part of the $P(E,E')$ function. The collisions that do exchange large amounts of energy are especially interesting from a chemical point of view because they are precisely the encounters that can energize molecules for subsequent chemical reactions. Of course, these make up only a fraction of all possible quenching processes. A much larger number of collisions involve only modest changes in the rotational and translational energies of the bath. In addition, a second mechanism has been identified in pyrazine/CO_2 collisions that results in vibrational (V → V) energy gain in the CO_2 bath. This process is mediated through long-range interactions and involves negligible rotational and translational excitation of CO_2. For donor energies near 40 000 cm^{-1}, the long-range V → V channel accounts for only a small fraction of the energy loss relative to the V → RT channel and does not involve the large changes in pyrazine energy that result from the V → RT pathway. In this paper, we explore whether a large energy V → RT relaxation mechanism is present when water is the collision partner and, if so, whether this pathway plays a significant role in the collisional relaxation of highly vibrationally excited molecules. We have focused our attention on rotational and translational energy gain in the vibrationless state of the bath, which, for hot pyrazine and CO_2, has been established as the primary deactivation pathway for donor energies near 40 000 cm^{-1}.

This paper reports the first state-resolved studies of energy gain in H_2O (000) following collisions with highly vibrationally excited pyrazine, where (000) indicates the ground vibrationless state of water. The overall experimental approach is similar to that for the pyrazine/CO_2 experiments[22,23] from our labs with a few notable exceptions. Highly vibrationally excited pyrazine is prepared in the gas phase with 37 900 cm^{-1} of internal energy by pulsed one-photon absorption of 266 nm light and rapid radiationless transitions to the ground electronic state.[26−28] The time for production of vibrationally hot, S_0 pyrazine is ∼50 ns. Collisions take place between highly excited pyrazine and a low-pressure, 300 K bath of water vapor, resulting in an energy gain in H_2O. It is known that pyrazine undergoes decomposition to form hot HCN fragments when excited with 248 nm light;[29] however, following 266 nm excitation, the fragmentation lifetime (∼60 μs) is much longer than our energy-transfer measurement times at 1 μs.[30] A detailed discussion of the implications that pyrazine fragmentation may have on our energy-transfer results has been presented previously.[23] The main conclusion of this discussion is that the lifetime measurements and the early time shape of our transient signals provide convincing evidence that highly vibrationally excited pyrazine is the energy source in the energy-transfer measurements presented here. Collisions that deposit energy into excited rotational states of H_2O (000) are investigated by monitoring the appearance of individual rotational quantum states of H_2O (000) using transient IR laser absorption of the strongly allowed (000) → (001) asymmetric stretch transition. The IR probe source is a commercial F-center laser operating at 2.7 μm that has been modified substantially to allow for single-mode continuous-frequency scans. When the appearance of individual states of H_2O (000) at short times following the excitation of pyrazine is recorded, information about the nascent distribution of the excited rotational states in H_2O (000) that result from single collisions with highly excited pyrazine is obtained. Measurements of Doppler-broadened transient absorption line profiles yield information on the distributions of translational energy for the excited rotational states investigated. In addition, absolute rate constants for energy gain in H_2O (000) are measured and probabilities are reported.

Experimental Section

The experiments were performed using a recently constructed transient absorption spectrometer operating at 2.7 μm, as shown in Figure 1. A 1:1 mixture of pyrazine and water vapor was introduced into a 250 cm flowing-gas collision cell maintained at a pressure of approximately 20 mTorr at 298 K. Highly vibrationally excited pyrazine was prepared in the cell by single-photon absorption of the quadrupled output at 266 nm of a Nd:YAG laser. The UV excitation source was operated at 10 Hz

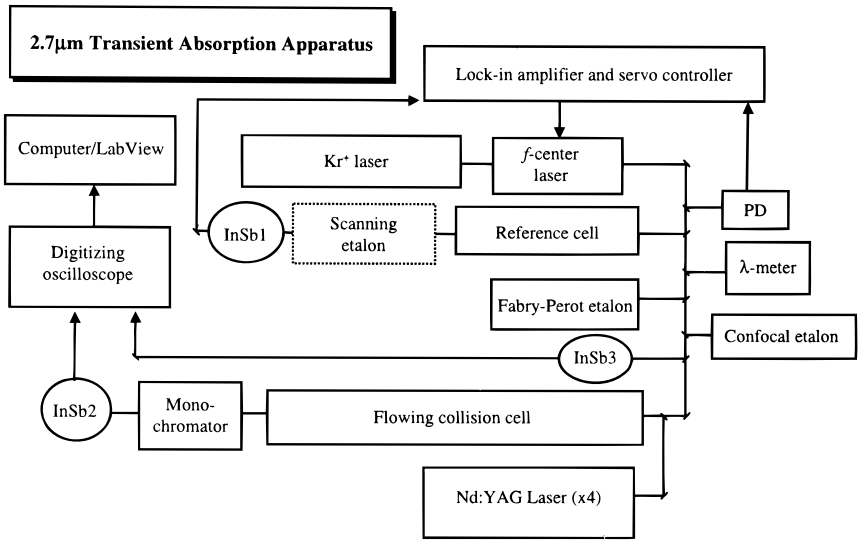

Figure 1. The 2.7 μm transient absorption spectrometer. A 1:1 mixture of pyrazine and H_2O are introduced into a 250 cm flowing-gas collision cell maintained at a pressure of approximately 20 mTorr at 298 K. The 266 nm quadrupled output of a pulsed Nd:YAG laser is used to prepare highly vibrationally excited pyrazine. Excited rotational states of H_2O (000) that are populated through collisions with hot pyrazine are probed by measuring the time-dependent changes in the transmitted intensity of a single-mode F-center laser. A full description of the F-center operation is presented in the text.

with a 6 ns pulse width. The repetition rate of the UV light was reduced to 1 Hz with a mechanical shutter to allow sufficient time to refresh the collision cell with pyrazine and water between laser shots. UV fluences were kept below 5 MW cm^{-2}, a regime in which power-dependent measurements on pyrazine display linear absorption. At the cell pressures used, the gas kinetic collision time is $\sim$4 μs.

Transient absorption measurements of water were performed using the tunable output of a single-mode F-center laser operating at $\lambda = 2.4-2.8$ μm. The F-center laser is pumped by the 674 nm output of a CW krypton ion laser. Single-mode frequency scanning of the F-center laser is achieved with an approach similar to that taken by Nesbitt and co-workers.[31] Coarse frequency selection is achieved with an intracavity diffraction grating and output of a single-cavity mode is accomplished using a scanning intracavity Etalon. This configuration results in a laser bandwidth of 0.0003 cm^{-1}. Infrared wavelength scanning is performed by angle-tuning a pair of intracavity CaF_2 plates while the intracavity Etalon is simultaneously scanned using active feedback to maintain single-mode operation. Frequency scans up to 0.4 cm^{-1} can be accomplished in this manner. A wavemeter is used to determine the IR wavelength to within $\pm$0.01 cm^{-1}.

To collect transient absorption data for individual rotational states of H_2O, the output of the F-center laser is actively locked to the absorption line of interest using an external reference feedback loop. A small frequency dither is induced in the IR output using an intracavity mirror mounted on a piezoelectric stack. Approximately 10% of the laser output is directed through a multipass cell containing up to 1 Torr of water vapor before it is collected on an indium antimonide detector (denoted InSb1 in Figure 1). For population measurements, the dither provides an error signal, which in conjunction with a lock-in amplifier, is used to lock the laser frequency to the peak of individual H_2O rotational lines. For Doppler-broadened transient line width measurements, the IR laser is locked to a fringe of a scanning confocal etalon and transient absorption measurements are collected as a function of the IR wavelength. A fixed-length confocal Etalon with a free spectral range of 0.0049 cm^{-1} is used to calibrate the IR frequency during line width measurements. Our experimental accuracy for line shapes was determined by measuring the line width of a 298 K CO_2 transition (P40, $00^00 \rightarrow 10^01$). Our experimental value of $\Delta\nu_{obs} = 0.0074$ cm^{-1} agrees well with the reported value of 0.0067 cm^{-1} and results in error bars of $\pm$0.001 cm^{-1} on line width measurements.

All transient absorption measurements are performed by monitoring the time-dependent variations in the transmitted IR intensity with respect to the pulsed excitation of pyrazine. The IR light transmitted through the collision cell is passed through a monochromator to remove unwanted UV light or residual red light from the krypton laser before it is collected on a liquid nitrogen cooled InSb detector (InSb2) and amplified. The combined rise time of the signal is 100 ns. The monochromator also discriminates effectively against IR emission from excited pyrazine that may interfere with absorption due to water. In any absorption measurement, the desired quantity is I_t/I_o, the fractional transmitted intensity. This is acquired in real time by collecting the transmitted IR intensity on a dc-coupled digital oscilloscope. The dc-coupled signal has contributions from changes in H_2O (000) populations (the desired signal) and from intensity fluctuations in the IR laser intensity. The measured signal is defined as $I_{DC} = I(t)T(t)$, where $I(t)$ is the incident IR laser intensity and $T(t)$ is the fractional transient transmission due to molecular absorption. To separate the desired intensity changes from the undesirable fluctuations, it is necessary to determine $I(t)$. This is accomplished by measuring the precell IR intensity on a matched detector/amplifier (InSb3). The precell signal is referred to as $I_{ref}(t)$ and is directly proportional to $I(t)$ so that $I_{ref}(t) = \gamma I(t)$, where γ is a constant scaling factor. The factor γ is determined for each transient measurement from the ratio of intensities prior to the UV excitation pulse, thus $\gamma = I_{DC}\ (t < 0)/I_{ref}\ (t < 0)$. To obtain the change in fractional transmitted intensity due to changes in the populations of H_2O (000) rotational states, $T(t)$ is calculated using the expression $T(t) = \{I_{DC}(t)\}/\{I_{ref}(t)/\gamma\}$ and then used in Beer's Law to calculate the transient number density of H_2O (000).

Research grade pyrazine (Aldrich, 99.9%) was used in these experiments after being degassed by several freeze/pump/thaw cycles. The water was distilled at 100 °C and collected directly in a vacuum flask to prevent absorption of atmospheric gases.

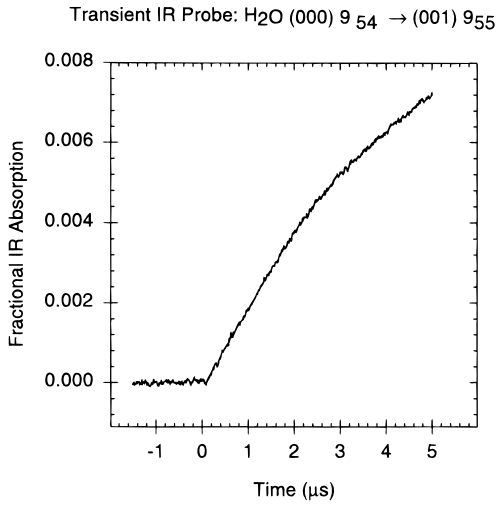

Figure 2. Fractional transient absorption of H_2O (000) $J_{K_aK_c} = 9_{54}$ resulting from collisions with highly excited pyrazine ($E_{vib} = 37\,900$ cm^{-1}) measured as a function of time following UV excitation of pyrazine. The collision cell pressure is 20 mTorr at 298 K, and the gas kinetic collision time is approximately 4 μs. Populations are measured at 1 μs, where the linear absorption signals correspond to population changes in H_2O resulting from single collisions with highly excited pyrazine. Typical transient signals result from averaging 200−300 laser UV laser shots.

Results

1. Rotational Excitation of H_2O (000). The appearance of population in more than 20 excited rotational states of H_2O (000) with $E_{rot} > 1000$ cm^{-1} was measured using transient IR absorption. For all absorption measurements, the IR probe was the strongly allowed asymmetric stretch (000) → (001) transition in H_2O. The transient absorption signal for the appearance of H_2O (000) $J_{K_aK_c} = 9_{54}$ is shown in Figure 2, with $t = 0$ corresponding to UV excitation of pyrazine. In labeling the rotational states of water, J is the total rotational angular momentum quantum number and K_a and K_c are the limiting symmetric top projection quantum numbers. Collisions resulting in energy-gain in H_2O (000) with $E_{rot} < 1000$ cm^{-1} were not included in our measurements because excessive IR absorption due to atmospheric water precludes energy-gain measurements for the lower energy states of water that are thermally populated at 300 K. Nascent populations of H_2O (000) in individual excited $J_{K_aK_c}$ states were obtained by measuring the transient absorption at 1 μs following pyrazine excitation and integrating over experimentally determined Doppler-broadened transient absorption line profiles (described below). Using Beer's Law and well-established oscillator strengths for water,[32] absolute populations were determined. The distribution of excited rotational states in H_2O (000) following collisions with highly vibrationally excited pyrazine is found by dividing the population in each state by its nuclear spin degeneracy[33] and plotting the natural log of this value as a function of the rotational energy. The results of this analysis are shown in Figure 3, and the distribution is well-described using Boltzmann statistics with $T_{rot} = 920 \pm 100$ K. This temperature is substantially larger than the initial rotational temperature of 300 K and shows that collisions between water and hot pyrazine can result in large rotational energy gains in H_2O (000), leaving water vibrationally unexcited but rotationally hot.

2. Nascent Recoil Velocities of Scattered H_2O (000). Transient Doppler-broadened line shapes for excited rotational states of H_2O (000) were measured in order to determine the distributions of recoil velocities that accompany energy gain into excited rotational states of H_2O (000). Populations of individual rotational levels were measured at 1 μs following pyrazine excitation and collected as a function of IR frequency shift $\delta\nu$ from the line center. The transient line shape for H_2O (000) $J_{K_aK_c} = 9_{54}$ is shown in Figure 4, along with a frequency calibration scan from a fixed-length confocal Etalon (FSR = 0.0049 cm^{-1}). The experimental data, shown as open circles,

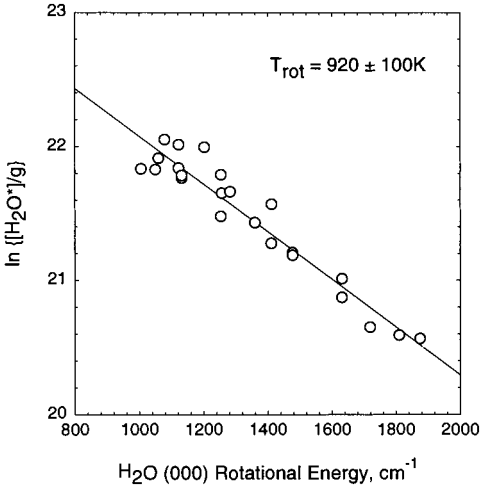

Figure 3. Distribution of nascent rotational states in H_2O (000) resulting from collisions with highly vibrationally excited pyrazine ($E_{vib} = 37\,900$ cm^{-1}). Populations have been measured at 1 μs following UV excitation of pyrazine under conditions in which the gas kinetic collision time is 4 μs. These data include rotational states with energies between 1000 and 2000 cm^{-1}. Populations of individual states have been divided by g, the nuclear spin degeneracy. The nascent rotational distribution is well described by a rotational temperature of $T_{rot} = 920 \pm 100$ K, indicating that substantial increases in the rotational energy of H_2O (000) accompany the collisional relaxation of highly excited pyrazine.

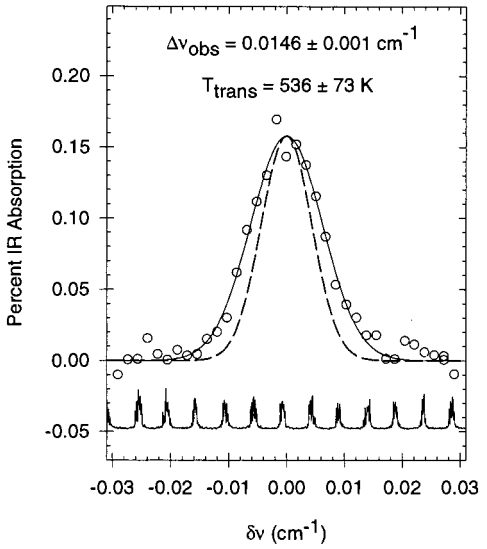

Figure 4. Transient absorption line shape for H_2O (000) $J_{K_aK_c} = 9_{54}$ collected at 1 μs following UV excitation of pyrazine. The transient absorption data are shown as open circles. The data are fit to a single Gaussian function, shown as a solid line. This fit yields a full width half-maximum of $\Delta\nu_{obs} = 0.0146 \pm 0.001$ cm^{-1}, which corresponds to a lab-frame translational temperature of $T_{trans} = 536 \pm 73$ K. The transient line shape is slightly broader than that for a 300 K distribution of translational energies, which is shown as a dashed line for comparison. Frequency calibration of the line widths is accomplished by recording the IR transmission through a confocal etalon having a free spectral range of 0.0049 cm^{-1} as the laser frequency is scanned across the line shape. The etalon signal is shown in the lower trace.

TABLE 1: Transient Absorption Line Widths for Rotational States of Water Populated from Collisions of the Type Pyrazine (E_{vib} = 37 900 cm^{-1}) + H_2O → Pyrazine ($E_{vib} - \Delta E$) + H_2O (000, $J_{K_aK_c}$, V)

H_2O (000) $J_{K_aK_c}$	E_{rot}, cm^{-1} [a]	ν_0, cm^{-1} [a]	$\Delta\nu_{obs}$, cm^{-1} [b]	T_{trans}, K[c]	$\langle E_{trans}\rangle_{lab}$, cm^{-1} [d]	$\langle \Delta E_{trans}\rangle_{rel}$, cm^{-1} [e]
7_{52}	1059.841	3553.74	0.0152 ± 0.001	635 ± 84	662 ± 87	430 ± 106
8_{44}	1131.776	3719.76	0.0143 ± 0.001	513 ± 72	535 ± 75	274 ± 91
9_{36}	1282.919	3666.08	0.0149 ± 0.001	574 ± 77	598 ± 80	351 ± 98
8_{62}	1411.647	3710.71	0.0148 ± 0.001	552 ± 75	576 ± 78	324 ± 95
9_{54}	1477.297	3716.16	0.0146 ± 0.001	536 ± 73	559 ± 77	303 ± 93
9_{63}	1631.384	3708.26	0.0148 ± 0.001	553 ± 75	577 ± 78	325 ± 95
10_{65}	1874.974	3706.55	0.0150 ± 0.001	569 ± 76	593 ± 79	345 ± 97

[a] Rotational energies and absorption frequencies at line center (ν_0) are from the 1996 HITRAN database (ref 32). [b] Transient absorption line widths are measured at 1 μs following UV excitation of pyrazine. Each line profile, such as the one shown in Figure 3, is fit to a Gaussian function, and the resulting full width half-maximum values ($\Delta\nu_{obs}$) are reported here. [c] The translational temperatures associated with individual rotational states of water are obtained using the expression $T(K) = \{mc^2\Delta\nu_{obs}^2\}/\{8R(\ln 2)\nu_0^2\}$, where m is that mass of water, c is the speed of light, $\Delta\nu_{obs}$ is the experimentally determined transient absorption line width, R is the molar gas constant, and ν_0 is the absorption frequency at the line center. [d] The mean lab frame translational energy of H_2O (000) molecules that are recoiling from highly excited pyrazine, calculated using $\langle E_{trans}\rangle_{lab} = 1.5k_BT_{trans}$. [e] The mean change in the relative translational energy of H_2O (000) and pyrazine resulting from collisions in the center of mass frame, calculated using $\langle \Delta E_{trans}\rangle_{rel} = \{(80 + 18)/80\}\langle \Delta E_{trans}\rangle_{lab} = 1.22\ \langle \Delta E_{trans}\rangle_{lab}$ and assuming the initial translational energy of H_2O (000) is 1.5 k_BT_0 = 310 cm^{-1} with T_0 = 300 K.

are fit to a Gaussian line shape using nonlinear least-squares analysis, the results of which are shown in Figure 4 as a solid line. Our line width data and limited polarization studies are consistent with isotropic distributions of scattered H_2O molecules, although low signal levels have precluded a complete polarization-dependent analysis. The resulting full width half-maximum for the 9_{54} state of H_2O (000) is $\Delta\nu_{obs} = 0.0146 \pm 0.001$ cm^{-1}, which corresponds to a translational temperature in the lab frame of $T_{trans} = 536 \pm 73$ K. The observed transient absorption line shape for the H_2O (000) 9_{54} state is broadened with respect to the 300 K line width of $\Delta\nu_{298} = 0.0104$ cm^{-1} (shown in Figure 4 as a dashed line), demonstrating that collisions resulting in rotationally hot H_2O (000) are accompanied by increased translational energies. The transient Doppler-broadened line widths for a number of rotationally excited H_2O (000) states are reported in Table 1 along with the lab frame translational temperatures. The average nascent translational energies in the lab frame are found using E_{trans}(lab) = $3/2k_BT_{trans}$(lab), where k_B is Boltzmann's constant. These values are presented in Table 1. As shown in Figure 5, the translational temperatures for H_2O (000) show little variation over the range of rotational energies investigated and there is no apparent correlation with E_{rot} or with the J, K_a, or K_c quantum numbers. The measured translational temperatures are all elevated somewhat relative to the initial 300 K velocity distribution, but it is noteworthy that the distributions of recoil velocities for the excited rotational states of H_2O (000) are much cooler than those seen in earlier quenching studies where CO_2 is the bath. Relative to quenching by CO_2, only a small amount of translational energy is imparted to H_2O (000) following collisions with vibrationally hot pyrazine. The implications of this result and a comparison with quenching by CO_2 will be discussed later in this paper.

3. Rotational Excitation Rates of H_2O (000). To obtain a more complete understanding of the collisional relaxation of vibrationally excited pyrazine by water molecules, we have measured absolute rates of appearance for the excited rotational states of H_2O (000). The transient absorption measurements such as shown in Figure 2 represent the appearance of a specific rotational state in H_2O (000) resulting from the process

$$\text{Pyr}\ (E_{vib} = 37\ 900\ \text{cm}^{-1}) + H_2O\ (300\ \text{K}) \rightarrow \text{Pyr}\ (E_{vib} - \Delta E) + H_2O\ (000, J_{K_aK_c}, V)$$

where Pyr denotes pyrazine, ΔE is the amount of energy lost from hot pyrazine via a collision with H_2O, and V is the recoil

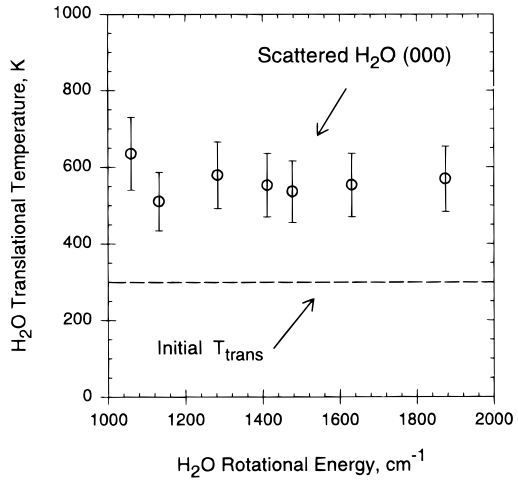

Figure 5. Nascent translational temperatures for individual rotational states of H_2O (000) having rotational energies E_{rot} = 1000−2000 cm^{-1}. The translational temperatures are determined by measuring the Doppler-broadened transient absorption line shapes at 1 μs following UV excitation of pyrazine. The distributions of recoil velocities associated with each rotational state have translational temperatures in the range 510−635 K and are only slightly more energetic than the initial 300 K velocity distribution. In addition, the final translational energy in water does not correlate with the rotational energy of H_2O (000) nor with the J, K_a, and K_c quantum numbers.

of H_2O (000) in the $J_{K_aK_c}$ state. The differential rate of appearance of individual rotational states of H_2O (000) can be written as

$$d[H_2O(J)]/dt = k_2^J[\text{Pyr*}][H_2O\ (300\ \text{K})]$$

where $[H_2O(J)]$ is the population of H_2O (000) in the $J_{K_aK_c}$ quantum state, t is the time following UV excitation of pyrazine, k_2^J is the bimolecular rate constant for appearance of the $J_{K_aK_c}$ state, [Pyr*] is the concentration of excited pyrazine molecules, and $[H_2O\ (300\ \text{K})]$ is the concentration of bulk water at 300 K. At short times relative to pyrazine excitation, the depletion of [Pyr*] and $[H_2O\ (300\ \text{K})]$ from their values at $t = 0$ is minimal. The concentrations at 1 μs are essentially the same is their values at $t = 0$, denoted respectively by $[\text{Pyr*}]_0$ and $[H_2O]_0$. Therefore, immediately following the UV excitation pulse, the rate of appearance of individual H_2O states is extremely well represented by

$$\Delta[H_2O(J)]/\Delta t = k_2^J[\text{Pyr*}]_0[H_2O]_0$$

TABLE 2: Rate Constants, Probabilities, and $\langle \Delta E \rangle$ Values for the Process Pyrazine ($E_{vib} = 37\,900$ cm^{-1}) + $H_2O \rightarrow$ Pyrazine ($E_{vib} - \Delta E$) + H_2O (000, $J_{K_aK_c}$, V)

$J_{K_aK_c}$	E_{rot}[a]	k_2^J[b]	prob$_{LJ}$[c]	$\langle \Delta E_{rot} \rangle$[d]	$\langle \Delta E_{total} \rangle$[e]
8_{36}	1006.116	$(8.1 \pm 2.4) \times 10^{-13}$	9.8×10^{-4}	693	1028
8_{35}	1050.158	$(3.4 \pm 1.0) \times 10^{-13}$	4.1×10^{-4}	737	1072
7_{53}	1059.647	$(2.9 \pm 0.9) \times 10^{-13}$	3.5×10^{-4}	747	1082
9_{18}	1079.080	$(9.0 \pm 2.7) \times 10^{-13}$	1.2×10^{-3}	766	1101
9_{28}	1080.386	$(2.1 \pm 0.6) \times 10^{-13}$	2.5×10^{-4}	767	1102
8_{45}	1122.709	$(7.6 \pm 2.3) \times 10^{-13}$	9.2×10^{-4}	810	1145
8_{44}	1131.776	$(2.2 \pm 0.7) \times 10^{-13}$	2.6×10^{-4}	819	1154
9_{27}	1201.922	$(6.9 \pm 2.1) \times 10^{-13}$	8.3×10^{-4}	889	1224
9_{37}	1216.232	$(1.7 \pm 0.5) \times 10^{-13}$	2.0×10^{-4}	903	1238
8_{54}	1255.167	$(5.1 \pm 1.5) \times 10^{-13}$	6.1×10^{-4}	942	1277
8_{53}	1255.913	$(2.2 \pm 0.7) \times 10^{-13}$	2.6×10^{-4}	943	1278
9_{36}	1282.919	$(5.4 \pm 1.6) \times 10^{-13}$	6.5×10^{-4}	970	1305
9_{45}	1360.235	$(4.8 \pm 1.4) \times 10^{-13}$	5.8×10^{-4}	1047	1382
8_{63}	1411.612	$(4.9 \pm 1.5) \times 10^{-13}$	5.9×10^{-4}	1099	1434
8_{62}	1411.647	$(1.4 \pm 0.4) \times 10^{-13}$	1.7×10^{-4}	1099	1434
9_{54}	1477.297	$(3.6 \pm 1.1) \times 10^{-13}$	4.3×10^{-4}	1164	1499
9_{64}	1631.251	$(1.1 \pm 0.3) \times 10^{-13}$	1.3×10^{-4}	1318	1653
9_{63}	1631.384	$(3.3 \pm 0.9) \times 10^{-13}$	4.0×10^{-4}	1318	1653
9_{72}	1810.589	$(2.5 \pm 0.7) \times 10^{-13}$	3.0×10^{-4}	1498	1833
10_{65}	1874.974	$(1.7 \pm 0.5) \times 10^{-13}$	2.0×10^{-4}	1562	1897

[a] The energy in cm^{-1} of the H_2O (000) rotational $J_{K_aK_c}$ state from ref 33. [b] Rate constants for appearance of H_2O (000) in state $J_{K_aK_c}$ resulting from collisions with highly excited pyrazine. All rate constants are in units of cm^3 molecule^{-1} s^{-1}. [c] The probability of energy gain into the $J_{K_aK_c}$ state of H_2O (000) within the Lennard-Jones collision model. [d] The mean change in H_2O (000) rotational energy in cm^{-1} for collisions that excite the $J_{K_aK_c}$ state. $\langle \Delta E_{rot} \rangle = E_{rot} - 1.5k_BT_0 = E_{rot} - 310$ cm^{-1} with $T_0 = 300$ K. [e] The mean total energy change in cm^{-1} associated with collisions that excite H_2O (000) in the $J_{K_aK_c}$ state. $\langle \Delta E_{total} \rangle = \langle \Delta E_{rot} \rangle + \langle \Delta E_{trans} \rangle_{rel}$, where $\langle \Delta E_{trans} \rangle_{rel} \approx 335$ cm^{-1} (see Table 1).

The appropriateness of this model at 1 μs is demonstrated by the linear early-time transient absorption signal shown in Figure 2. Data collection at 1 μs occurs prior to the average gas kinetic collision time and the diffusion time out of the IR probe volume. To solve for k_2^J, the remaining parameters are determined experimentally. [$H_2O(J)$] is determined from the fractional transient absorption at Δt using well-established oscillator strengths for water transitions.[32] [Pyr*]$_0$ is determined by measuring the UV absorption of pyrazine and dividing by the laboratory interaction volume. [H_2O]$_0$ is determined by measuring the IR absorption of a thermally populated water state in the collision cell prior to UV excitation and relating the fractional absorption to concentration using Beer's Law. Energy-transfer rate constants for excitation of rotationally hot H_2O (000) have been determined in this way and are reported in Table 2. Note that the rate constants reflect the 3:1 nuclear spin statistics for odd/even symmetries of water rotational states.[33]

It is useful to consider the likelihood of energy gain into individual final quantum states of water. The probability for energy transfer is readily obtained from our data by dividing the energy-transfer rate constants for energy gain into individual bath states of H_2O by the collision rate constant. At this point, one must decide on the appropriate model for molecular collisions. The hard-sphere collision model for pyrazine and water has a rate constant of $k_{HS} = 3.3 \times 10^{-10}$ cm^3 molecule^{-1} s^{-1}. This corresponds to a hard-sphere energy-transfer probability (P_{HS}) for appearance of the $J_{K_aK_c} = 9_{18}$ state of H_2O (000) of $P_{HS} = 2.7 \times 10^{-3}$, meaning that excitation of the 9_{18} state, for example, occurs once for every 370 hard-sphere gas kinetic collisions. Using the Lennard-Jones collision rate constant for pyrazine and water of $k_{LJ} = 8.3 \times 10^{-10}$ cm^3 molecule^{-1} s^{-1}, the Lennard-Jones probability (prob$_{LJ}$) for the 9_{18} state is reduced to $P_{LJ} = 1.1 \times 10^{-3}$, corresponding to energy transfer once every 920 collisions. Probabilities for energy transfer into excited $J_{K_aK_c}$ states of H_2O (000) have been determined from our data using the more realistic Lennard-Jones collision model and are presented in Table 2. It should be noted that the two collision models considered here have collision rate constants that differ by a factor of 2.5. This difference is reflected directly in the corresponding probabilities, so caution must be exercised when comparing energy-transfer probabilities for different collision partners or from different studies. In using the Lennard-Jones collision model for pyrazine/water energy transfer, the reported probabilities are less than those obtained with the hard-sphere model.

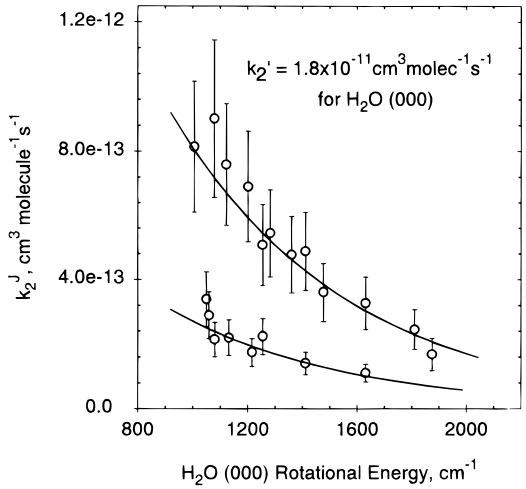

Figure 6. Absolute rate constants for appearance of individual rotational states of H_2O (000) as a function of rotational energy. The open circles are determined from transient absorption measurements as described in the text and include contributions from the experimentally measured Doppler-broadened line widths. The solid lines are calculated from the rotational temperature of the H_2O (000) rotational distribution, shown in Figure 3. The rate constants fall into two distinct curves due to the 3:1 nuclear spin statistics of water. An integrated rate constant for rotational and translational energy gain in H_2O (000) is determined by summing over all rotational states with energies between 1000 and 2000 cm^{-1}. This yields an integrated rate constant $k_2' = (1.8 \pm 0.5) \times 10^{-11}$ cm^3 molecule^{-1} s^{-1}.

It is informative to determine an integrated rate constant to assess the contribution of high-energy rotational and the accompanying translational excitation in H_2O (000) to the overall collisional relaxation of highly excited pyrazine. The integrated rate constant, k_2', for appearance of final water states with $E_{rot} > 1000$ cm^{-1} is found by determining rate constants for each rotational state of H_2O (000) from the experimentally measured rate constants (Table 2) and rotational distribution (Figure 3). For the even and odd symmetry states of water, Figure 6 shows the rate constants (open circles) and the associated rotational distributions (solid lines). The rate constants are then summed together, and the integrated rate constant is found using $k_2' = \Sigma k_2^J$, where the summation is over all rotational levels in the (000) vibrationless state. For postcollision rotational states of water with $E_{rot} > 1000$ cm^{-1}, the integrated rate constant has a value for $k_2' = (1.8 \pm 0.5) \times 10^{-11}$ cm^3 molecule^{-1} s^{-1}. It is reasonable to assume that some amount of energy is lost from hot pyrazine on every collision, so the collision rate is an upper limit for the energy loss rate. Therefore, the fraction of collisions that involve large changes in rotational energy in the bath (corresponding in our measurements to water states with $E_{rot} > 1000$ cm^{-1}) is given by an integrated probability prob$' = k_2'/k_{LJ} = 2.2 \times 10^{-2}$. This means that one out of 46 Lennard-Jones collisions between water and hot pyrazine results in a substantial increases in water's rotational energy. This is a small fraction of all possible energy-

transfer events, but it is significant because it corresponds to the high-energy tail of $P(E,E')$ for relaxation of excited pyrazine through collisions with water. It should be noted that the integrated probability given here represents a lower limit to the contribution of the entire V → RT relaxation channel since our data is a measure of large ΔE collisions. We expect that collisions involving small changes in bath rotation will contribute significantly to the overall probability, but the transient IR probe technique used in these studies is not suited for unambiguously measuring small ΔE collisions for two reasons. The first reason is that the low-energy states of water are initially populated at 300 K and acquiring transient absorptions signals associated with these states requires measuring small changes in intensity that ride on top of large absorptions due to the ambient population. The second problem is in identifying the source of the population change for a given state. For states that are substantially populated at 300 K, the changes in transient absorption for a particular quantum state can result both from depletion of that state and simultaneous production through collisions with other initial states. The overall changes are very well determined in our measurements, but the branching ratio between appearance and depletion is not. On the other hand, for higher energy rotational states that have negligible populations at 300 K and therefore negligible background IR absorption, there is no ambiguity in the meaning of the absorption changes. Higher energy rotational states with $E_{rot} > 2000$ cm^{-1} are also not included in the integrated rate constant because, for those energies, no population changes were detectable within our current experimental sensitivity. As such, these energy-transfer events represent a smaller contribution to the integrated rate than do the lower values of E_{rot}.

Discussion

The experimental results reported here provide one of the first opportunities for characterizing the "strong" (i.e., large ΔE) collisions between highly excited pyrazine and water. The transient IR absorption technique allows us to measure independently the partitioning of energy gain into different degrees of freedom in the bath molecules and the absolute rate constants for such processes. These experiments have been designed to focus only on those collisions that populate rotationally excited water states. Ideally, we would like to characterize both the "weak" (i.e., those with small ΔE values) and "strong" collisions, but this would necessitate characterizing the entire energy-transfer distribution function. As discussed in the previous section, there are a number of experimental difficulties in cleanly characterizing the small ΔE collisions. On the other hand, our measurements of collisions that involve large ΔE values are relatively straightforward to interpret, since they arise from the appearance of water molecules in well-defined quantum states following collisions with hot pyrazine. One of the advantages of the IR probe technique is that the results reported up to this point are free from any assumptions about branching ratios or initial populations. The meaning of the results presented so far is clear. Water molecules undergo collisions with vibrationally hot pyrazine, and a subset of these collisions result in rotationally hot ($T_{rot} = 920$ K) but vibrationally unexcited H_2O (000) molecules. The rotational excitation is accompanied by moderate translational excitation of H_2O (000). For H_2O (000) with nascent rotational energies $E_{rot} > 1000$ cm^{-1}, this type of V → RT energy transfer occurs about once for every 46 Lennard-Jones collisions. Beyond these observations, it is interesting to consider how the observed energy gains into rotation and translation of water correlate with energy losses from the hot pyrazine donor. To do this, it is necessary to consider the changes in rotational and translational energy of H_2O (000) in the center of mass reference frame. In the following sections, we discuss how ΔE values for the various degrees of freedom can be obtained from our data. We then compare the results for the V → RT energy gain in water to those for a CO_2 bath, and finally, we discuss possible mechanisms for the observed rotational and translational excitation of H_2O (000).

1. Magnitude of Energy Transferred from Hot Pyrazine to H_2O (000). The postcollisional energies of water molecules that take away energy from hot pyrazine are known extremely well in our experiments. The nascent rotational energies for scattered water molecules are the energies of the lower state of each IR probe transition. The nascent velocity distribution for each rotational state is determined from the Doppler-broadened line shape. To see how these results correspond to energy lost from hot pyrazine, it is necessary to determine the *changes* in energy associated with the rotational and translational excitation of H_2O (000). We first consider the mean increase in H_2O translational energy for the rotational states investigated. Table 1 lists the translational temperatures and mean kinetic energies in the lab frame for a number of rotational states in water. The quantities of interest for determining energy loss magnitudes are the velocity distributions in the center of mass reference frame, since they include the translational recoil of both pyrazine and water after collisions.[17] The lab frame velocity $\mathbf{v}_i$ for each species i is related to the velocity of the center of mass $\mathbf{V}$ and the center of mass velocity $\mathbf{w}_i$ for each species i by the equation

$$\mathbf{v}_i = \mathbf{V} + \mathbf{w}_i$$

Assuming an isotropic distribution of laboratory velocities, the mean square velocities in the lab and center of mass reference frames are related by

$$\langle \mathbf{v}_i \rangle^2 = \langle \mathbf{V} \rangle^2 + \langle \mathbf{w}_i \rangle^2$$

The relative velocity $\mathbf{v}_{rel}$ between pyrazine and water is given by

$$\mathbf{v}_{rel} = \mathbf{w}_{H_2O} + \mathbf{w}_{pyr}$$

and the total relative kinetic energy is given by

$$E_{rel} = \frac{1}{2}\mu \mathbf{v}_{rel}^2$$

where μ is the reduced mass of pyrazine and water. The center of mass velocity of water is related to the relative velocity by conservation of linear momentum with the equation

$$\mathbf{w}_{H_2O} = (m_{pyr}/M_{total})\mathrm{v}_{rel}$$

where m_{pyr} is the mass of pyrazine and M_{total} is the total mass of pyrazine and water ($M_{total} = 98$ g/mol). The lab frame velocity of water prior to the collision can be written in terms of the relative velocity,

$$\langle \mathbf{v}_{H_2O} \rangle^2 = \langle \mathbf{V} \rangle^2 + \langle \mathbf{v}_{rel} \rangle^2 (m_{pyr}/M_{total})^2$$

A similar expression can be written for the lab frame velocity of water after the collision

$$\langle \mathbf{v'}_{H_2O}\rangle^2 = \langle \mathbf{V}\rangle^2 + \langle \mathbf{v'}_{rel}\rangle^2 (m_{pyr}/M_{total})^2$$

Note that for collisions that exchange energy but do not involve changes in the masses of the collision partners, the velocity of the center of mass **V** does not change during the collision. Therefore, the change in relative translational energy resulting from a collision is given by

$$\langle \Delta E_{trans}\rangle_{rel} = \frac{1}{2}\mu\{\langle \mathbf{v'}_{rel}\rangle^2 - \langle \mathbf{v}_{rel}\rangle^2\}$$

which can also be written as

$$\langle \Delta E_{trans}\rangle_{rel} = \frac{1}{2}\mu(M_{total}/m_{pyr})^2\{\langle \mathbf{v'}_{H_2O}\rangle^2 - \langle \mathbf{v}_{H_2O}\rangle^2\}$$

This simplifies to

$$\langle \Delta E_{trans}\rangle_{rel} = \frac{1}{2}m_{H_2O}(M_{total}/m_{pyr})\{\langle \mathbf{v'}_{H_2O}\rangle^2 - \langle \mathbf{v}_{H_2O}\rangle^2\}$$

which reduces further to

$$\langle \Delta E_{trans}\rangle_{rel} = (M_{total}/m_{pyr})\langle \Delta E_{trans}\rangle_{lab} = 1.22\langle \Delta E_{trans}\rangle_{lab}$$

The change in translational energy in the lab frame is thus related to the change in kinetic energy in the center of mass reference frame. The *final* kinetic energy of scattered water molecules in the lab frame is known from our Doppler-broadened line shapes. The *initial* translational energy of molecules scattered into a particular final $J_{K_aK_c}$ state is not known precisely but can be defined using an initial velocity distribution with temperature T_0 such that

$$\frac{3}{2}k_B T_0 = \frac{1}{2}m_{H_2O}\langle \mathbf{v}_{H_2O}\rangle^2$$

To solve for the relative change in kinetic energy, some assumption must be made about the value of T_0. Numeric values for $\langle \Delta E_{trans}\rangle_{rel}$ have been calculated using $T_0 = 300$ K, which is the ambient temperature prior to collisions between hot pyrazine and water. These values are presented in Table 1 for each transient line width measured.

In a similar way, the change in rotational energy for the scattered water molecules is given by the difference between final and initial energies. The final energies E_{rot} are known exactly for each rotational state probed, but the exact initial rotational energies are not selected in our experiments. The mean initial rotational energy can be defined using an initial rotational temperature $T_0(J)$ so that the mean change in rotational energy can be written as

$$\langle \Delta E_{rot}\rangle = E_{rot} - \frac{3}{2}k_B T_0(J)$$

To determine ΔE_{rot}, it is necessary to make some assumption about $T_0(J)$. Numerical values for $\langle \Delta E_{rot}\rangle$ have been determined using $T_0(J) = 300$ K, the ambient temperature prior to collisions with excited pyrazine. Values for $\langle \Delta E_{rot}\rangle$ are shown in Table 2. Values for the mean total energy loss $\langle \Delta E_{total}\rangle$ from pyrazine associated with energy gain into the nascent rotational states of water studied are shown in Table 2 and result from summing the average rotational and translational energy changes for each final water state. The observed line widths from Table 1 display little variation over the range of rotational states studied, and they correspond to an average energy change of $\langle \Delta E_{trans}\rangle_{rel} \approx 335$ cm^{-1}. This average value has been used for calculating $\langle \Delta E_{total}\rangle$ values in Table 2. The choice of initial translational and rotational temperatures, T_0 and $T_0(J)$, has a direct impact on the resulting $\langle \Delta E\rangle$ values. The implications of our assumptions will be discussed in a later section.

It is quite interesting that the energies lost from hot pyrazine in a collision with water that excite rotational states in H_2O (000) with $E_{rot} > 1000$ cm^{-1} represent a small fraction of pyrazine's 37 900 cm^{-1} of available internal energy. In addition, these energy-transfer events do not occur very often. For example, the average energy loss from pyrazine associated with collisional excitation of H_2O (000) $J_{K_aK_c} = 10_{65}$ is $\langle \Delta E_{total}\rangle \approx 1900$ cm^{-1}, with 80% of the energy going into H_2O rotation, but our rate constant measurements reveal that excitation of this state occurs only once in every 5000 collisions. Therefore, statistically speaking, excitation of the 10_{65} state accounts for energy loss from hot pyrazine of only 0.38 cm^{-1} *per collision* of pyrazine with water. Since many final rotationally excited states of water are possible, it is useful to sum over the rotationally excited states of H_2O (000) that comprise the high-energy tail of $P(E,E')$, interpolating for states that were not measured directly. For final states with $E_{rot} > 1000$ cm^{-1}, the total energy lost from pyrazine that goes into H_2O (000) rotational and translational excitation is only $\sim$30 cm^{-1} per collision. Technically, this value is a lower limit, since the energy transfer into rotational states of water with $E_{rot} > 2000$ cm^{-1} is not included in the sum, but the probabilities for energy transfer into these states decrease rapidly with increasing rotational energy, so their contribution to the overall relaxation should be negligible. It is quite interesting to compare this result with total energy loss measurements in order to establish the relative importance of the high-energy V $\rightarrow$ RT energy-transfer channel. Unfortunately, bulk pyrazine/water relaxation data are not available, so a direct comparison is not possible. Collisional quenching data for vibrationally excited pyrazine[34] and benzene,[35] however, often yield similar average energy loss values, especially for polyatomic bath molecules (such as CO_2, CH_4, NH_3, and SF_6). Therefore, data for the benzene/water system should provide a reasonable estimate of the total average energy loss from hot pyrazine. The energy loss data indicate that benzene with $E_{vib} = 24\,000$ cm^{-1} transfers 373 cm^{-1} on average per collision with water. At the excitation energies used in our experiments, the average energy loss value should be even larger. The rotational and translational excitation of H_2O (000) that accompanies large ΔE collisions accounts for only a small fraction of the total average energy lost from pyrazine per collision with water.

It is important to recognize that the $\langle \Delta E_{rot}\rangle$ and $\langle \Delta E_{trans}\rangle_{rel}$ values reported in Tables 1 and 2 have been calculated assuming that, prior to undergoing a collision with hot pyrazine, the water molecules have initial energies near the mean of 300 K rotational and translational distributions. It is possible that the H_2O (000) molecules probed in our experiments actually originate from the high-energy tail of the 300 K Boltzmann distribution and have initial energies that are higher than the mean of a 300 K distribution. Most of the water molecules in the initial bath certainly have initial energies near the mean energy, and the number density decreases sharply with increasing energy. This factor will favor energy transfer involving molecules with energies near the mean. In contrast, the likelihood of rotational excitation is expected to increase for smaller changes in angular momentum, and this propensity would favor the precollision molecules that are from the high-energy tail of the initial rotational distribution. Translational excitation in the scattered water is also expected to be enhanced by higher initial collision

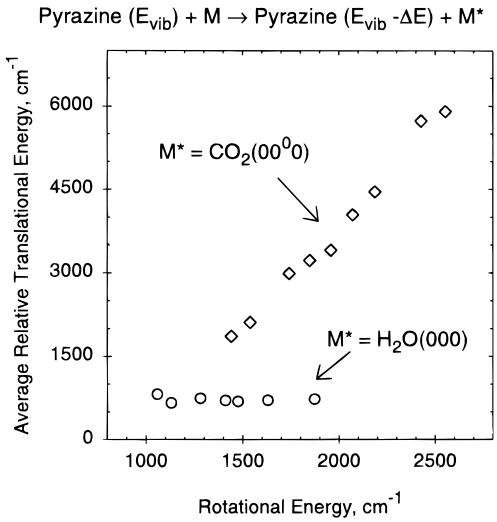

Figure 7. Comparison of average relative translational energies for H_2O (000) and CO_2 (00^00) (from ref 23), in the center of mass reference frame, resulting from collisions with highly excited pyrazine (E_{vib} = 37 900 cm^{-1}). The average translational energy is determined using $\langle E_{trans}\rangle_{rel} = \{(m_{pyr} + m_M)/m_{pyr}\}\{1.5k_B(T_{trans})_{lab}\}$, as described in the text. Notably, the nascent translational energies for H_2O (000) are only slightly greater than the precollision relative energies, and they do not correlate with the final rotational energy of H_2O (000) or with the J, K_a, or K_c quantum numbers. This is in marked contrast to the quenching behavior associated with CO_2 (00^00), in which the scattered CO_2 (00^00) molecules have translational energies that are characterized by translational temperatures as high as 4000 K and correlate directly with rotational energy.

velocities, although only modest recoil velocities were found for the rotational states studied, so this probably has little impact on the initial velocity distribution. It is clear from these considerations that the $\langle\Delta E\rangle$ values reported are best interpreted as upper limits.

2. Comparison of H_2O and CO_2 as Quenchers of Vibrationally Excited Pyrazine. It is quite informative to compare our results for water as a collisional quencher of vibrationally excited pyrazine with earlier studies from this lab[23] that used CO_2 as a collision partner with pyrazine excited at 266 nm. Our transient absorption measurements reveal that both H_2O (000) and CO_2 (00^00) can undergo substantial rotational excitation after a single collision with pyrazine containing E_{vib} = 37 900 cm^{-1}. The nascent rotational temperature of T_{rot} = 920 K for H_2O (000) rotational states with E_{rot} = 1000−2000 cm^{-1} is comparable to T_{rot} = 1200 K for the nascent distribution of CO_2 (00^00) states with E_{rot} = 1250−2800 cm^{-1}. For both H_2O and CO_2 baths, collisions that result in excited rotational levels of the vibrationless bath state also put energy into translation between hot pyrazine and the bath molecule. The average nascent relative translational energies of CO_2 (00^00) and H_2O (000) are shown in Figure 7 as a function of the rotational energy. For H_2O (000), the relative translational energy between collision partners is fairly small, with only ∼335 cm^{-1} being deposited into the center of mass kinetic energy from the vibrationally hot pyrazine. In addition, the translational energy gain for H_2O (000) rotational levels with E_{rot} > 1000 cm^{-1} does not correlate with the final rotational state. This is in marked contrast to the translational energy gain that is observed for rotationally excited CO_2 (00^00) after collisions with hot pyrazine. For collisions that result in the high J states of CO_2 (00^00), relative translational energy gains of 1000−6000 cm^{-1} are reported and the magnitude of the translational energy gain increases monotonically with the postcollision rotational state of CO_2. These large increases in relative translation between pyrazine and CO_2 (00^00) J = 56−84 result in $\langle\Delta E_{total}\rangle$ values for individual CO_2 states that are much larger than those seen for the high-energy rotations of H_2O (000). The relatively small recoil velocities of rotationally excited H_2O (000) highlight dynamic differences in the relaxation mechanisms, which will be discussed in the next section.

The state-resolved energy gain data reported here provide one of the first opportunities for comparing the details of the energy transfer that makes up the high-energy tail of $P(E,E')$ for different bath species. We now consider the extent to which the high-energy part of $P(E,E')$ that does not include vibrational excitation of the bath contributes to the overall energy loss from hot pyrazine. We have found that excitation of rotationally excited H_2O (000) states with E_{rot} > 1000 cm^{-1} accounts for average energy losses from pyrazine of ∼30 cm^{-1} per collision. A similar calculation for collisions that result in CO_2 (00^00) with E_{rot} = 1250−2800 cm^{-1} yields an average energy loss from pyrazine of ∼150 cm^{-1} per collision, with the largest contribution coming from vibration-to-translation energy transfer. Thus, the V → RT relaxation channel that results in the rotationally excited states of CO_2 (00^00) is more effective at cooling hot pyrazine than is the equivalent channel that results in rotationally excited H_2O (000). It is also interesting to note that relative to the overall average energy loss measurements, the high-energy part of $P(E,E')$ for water is even less important to the relaxation of pyrazine than in the case of CO_2. We can use the average energy loss data for benzene as a model for pyrazine relaxation. These data indicate that benzene with E_{vib} = 24 000 cm^{-1} transfers 373 cm^{-1} on average per collision with H_2O, while for a CO_2 bath, only 208 cm^{-1} are transferred on average. While our data for H_2O (000) and CO_2 (00^00) energy gain result from pyrazine molecules with higher internal energy, it is clear that the high-energy tail of $P(E,E')$ for H_2O (000) is negligible, while for CO_2 (00^00), the high-energy collisions contribute substantially to the overall relaxation. This result is somewhat surprising when it is considered that water is a better overall quencher of highly vibrationally excited benzene relative to CO_2. However, the results reported here highlight the differences in the shapes and magnitudes of the high-energy (i.e., supercollision) tail of the energy-transfer distribution functions for the bath gases. It is known that collisions with vibrationally hot pyrazine result in vibrational excitation of CO_2, but the accompanying rotational and translational energy gain is negligible so that the contribution of the V → V channel to the pyrazine/CO_2 system is minimal. It is not yet known whether vibrational energy gain in water will involve substantial rotational and translational excitation. However, we conclude that *vibrational* excitation of H_2O as well as rotational/translational excitation of the *low-energy rotational states* of H_2O (000) must be important in water's overall ability to quench highly vibrationally excited molecules. Experiments to measure collisions that excite vibrations in water are currently underway in our laboratories.

3. Mechanism for Rotational and Translational Excitation in H_2O (000). Our transient absorption measurements on the rotational and translational energy gain in the ground vibrationless state of H_2O following collisions with highly vibrationally excited pyrazine have revealed some very interesting and unusual results. Notably, a considerable amount of rotational excitation is found in H_2O (000) but only minimal translational excitation is associated with states having high rotational energies. In addition, the nascent distributions of H_2O (000) translational energies show little variation for the final

rotational states investigated. These results imply that the collisions responsible for energy gain in rotation and translation of H_2O (000) preferentially involve the hydrogen atoms on water and not the oxygen center. This is understood by recognizing that the center of mass in water is located very near the center of the oxygen atom. Thus, a direct hit on the oxygen atom has no means to provide torque on the water molecule and this type of collision would result in large recoil velocities between the collision partners with very little rotational excitation imparted. In contrast, essentially every hit on hydrogen, with the exception of a direct collision that occurs simultaneously along both O−H bond axes, is capable of producing rotational excitation in water. Because the hydrogen mass is so small, the moment of inertia of the water molecule is small, and therefore collisions with the hydrogen atoms result preferentially in enhanced rotational angular momentum rather than linear momentum in the water molecule.

We now consider several potential reasons for the observed relaxation behavior of highly excited pyrazine with H_2O. One possibility is that attractive interactions between pyrazine and water lead to orientation of water as the collision partners approach. Water has a large dipole moment ($\mu = 1.8$ D), which leaves the hydrogen atoms with partial positive charges. Thus, the most favorable interaction between pyrazine and water occurs with the hydrogen atoms closest to pyrazine. This interaction is particularly attractive in light of pyrazine's electron-rich π-cloud and axial lone pairs on the nitrogen atoms, and this is reflected in the Lennard-Jones well depth of 809 cm^{-1}. In the limit of low-velocity collisions, the most favorable electrostatic orientation of the water can be achieved during its approach to pyrazine, which would result in nearest approach of the hydrogen atoms. This mechanism is consistent with the modest recoil velocities that are observed, since orientation of the hydrogen atoms toward pyrazine would shield direct hits on the water center of mass. In contrast, it is noteworthy that, for collisions of pyrazine and CO_2, where large amounts of recoil are observed, the interaction well depth is only 195 cm^{-1}.

Another factor to consider in the collision dynamics of water with hot pyrazine is the time scale of molecular rotation relative to the duration time of a collision. At 300 K, the average relative velocity between pyrazine and water is $\langle v \rangle = 660$ m s^{-1}, and if the collision distance is defined using the Lennard-Jones well width, which we estimate at $d \approx 6$ Å, then the average duration of a collision is 0.92 ps. The rotational frequency ω of water at 300 K can be determined for rotation about each principal axis using $\langle E \rangle_{rot} = {}^1/_2 I\omega^2 = {}^1/_2 k_B T$, where I is the average of the moments of inertia I_A, I_B, and I_C along the A, B, and C axes and ω has units of rad s^{-1}. Solving for ω and dividing by 2π yields a rotational frequency $\nu = 2.3 \times 10^{12}$ rotations s^{-1}. Multiplying the collision time (0.92 ps/collision) by the rotational frequency, ν, reveals that water undergoes 2.1 rotations per collision on average. It is quite interesting to compare this result with a similar calculation for CO_2/pyrazine collisions. At 300 K, the average relative velocity for pyrazine and CO_2 is $\langle v \rangle = 470$ m s^{-1} and an average collision time is 0.85 ps if the Lennard-Jones well width is estimated at $d \approx 4$ Å. At 300 K, the rotational frequency for CO_2 is 3.8×10^{11} rotations s^{-1}, indicating that CO_2, on average, undergoes only 0.3 rotational cycles per collision. The picture that emerges is of water rotating several times during an encounter with hot pyrazine while CO_2, with its larger moment of inertia, does not even complete one rotational cycle. With water's center of mass almost on the center of the oxygen atom, molecular rotation of an approaching water molecule will involve the hydrogen atoms making the closest approach to pyrazine. In addition, the hydrogen atoms will present themselves several times during a collision. Taken together, these factors increase the probability that the hydrogen atoms in water will participate in the collision with hot pyrazine and lead to rotational, not translational, excitation of water. On the other hand, the large moment of inertia for CO_2 makes the time scale for CO_2 rotation longer than the typical collision time. This fact, along with the dumbbell shape of CO_2, makes it possible for both rotational and translational excitation to occur.

We plan to test these ideas by performing additional experiments on energy gain in H_2O (000) following collisions with hot pyrazine. Temperature-dependent experiments will test the importance of the electrostatic orientation model. This model predicts that, at reduced initial thermal energy, more efficient orientation will occur, resulting in enhanced rotational excitation without excessive Doppler line-broadening. As the initial thermal energy is increased, electrostatic orientation will compete with thermal kinetic energy, making orientation less likely and increasing the likelihood of a collision with the oxygen atom in water. This would cause more energy to be partitioned into the translational motion of water, and our transient absorption signals should exhibit an increase in their Doppler-broadening. The rotational time scale model, however, predicts that the rotational excitation of water should be essentially independent of temperature. The number of rotations per second will increase as $(T)^{1/2}$, but the collision time, which is inversely proportional to the average velocity, scales as $(T)^{-1/2}$. Since the number of rotations per collision is the product of the rotational frequency and the collision time, this quantity will remain invariant to temperature. Additional experiments are planned to clarify the role of molecular rotations in the collisional relaxation of hot pyrazine. We plan to use D_2O as a quenching gas instead of H_2O, thus reducing the number of rotations as the collision partners approach without substantially changing the mass of the quencher. It will also be possible to test for effects resulting from the rotational time scale model by measuring recoil velocities of H_2O (000) in low J states. The lower J states of water have a smaller number of rotations per collision, and it is anticipated that more collisions would involve the oxygen atom of water. Thus, the probability of translational excitation should increase, accompanied by minimal rotational energy gain. This effect would be observed as broadening in the transient Doppler line shapes for the low rotational levels of water.

Summary

In summary, we have reported the first rotationally resolved study of collisional energy transfer from a highly vibrationally excited aromatic donor to a water bath. These studies have investigated the nascent energy gain in the rotational and translational degrees of freedom in H_2O (000) that results from collisions with highly excited pyrazine having $E_{vib} = 37\,900$ cm^{-1}. Previous studies that focused on donor energy loss have shown that the overall quenching efficiencies are greater for water than for CO_2 as a bath. The goal of the present study was to investigate the means by which large ΔE energy transfer via the V → RT channel contributes to the overall relaxation of hot pyrazine through collisions with water. With respect to our experiments, there are three factors that contribute to the overall quenching efficiency of a given excited donor molecule. They are the magnitude of the energy transferred into a specific bath state in a successful collision, the probability that such an event occurs, and the number of acceptor states into which energy

can be transferred. Our measurements reveal that collisions between highly excited pyrazine and water can result in H_2O molecules with large amounts of rotational energy but that this rotational excitation is accompanied by only a small amount of translational energy. Thus, the amounts of energy lost from pyrazine in the V → RT energy-transfer channel are relatively small, especially when compared to the equivalent channel in CO_2 (00^00), which is characterized by a substantial high-energy tail in $P(E,E')$. The primary reason for the reduced energy-transfer magnitude is that the translational component of energy gain in H_2O (000) is much smaller that than for CO_2 (00^00). We attribute the lack of large recoil velocities in the H_2O (000) scattering to a combination of intermolecular attraction and mass effects and we conclude that the greater overall efficiency of water as a quencher of vibrationally excited molecules must involve channels other than the one investigated here. This highlights a key finding of this study, namely, that large ΔE collisions are not associated with the V → RT relaxation channel in pyrazine/H_2O energy transfer. Instead, the importance of the V → RT channel depends on molecular details of the bath and its interactions with the excited donor. Experiments are currently in progress in our laboratories to determine which molecular features of the bath control large ΔE energy loss processes from highly excited molecules.

Acknowledgment. We thank Professor W. Carl Lineberger for the generous use of an F-center laser and Dr. Bill Chapman for sharing his expertise in F-center laser techniques. We acknowledge Professor John Fourkas for advice in analysis of IR background corrections. We also thank Professors George Schatz, Raphy Levine, and David Coker for many fruitful and insightful discussions. A.S.M. is supported by a Clare Boothe Luce Professorship from the Henry Luce Foundation. M.F. was supported in part by funds from ACS-PRF Grant 29264-G6 and NSF Research Planning Grant CHE-9510485. Research support comes from NSF Grant CHE-9624533 with equipment support from ONR Grant N00014-96-1-0788.

References and Notes

(1) Tardy, D. C.; Rabinovitch, B. S. *Chem. Rev.* **1977**, *77*, 369.
(2) Krajnovich, D. J.; Parmenter, C. S.; Catlett, D. L. *Chem. Rev.* **1987**, *87*, 237.
(3) Gordon, R. J. *Comments At. Mol. Phys.* **1988**, *21*, 123.
(4) There are many excellent examples in the following: *Highly Excited Molecules: Relaxation, Reaction and Structure*; Mullin, A. S., Schatz, G. C., Eds.; American Chemical Society: Washington, DC, 1997.
(5) Cottrell, T. L.; McCoubrey, J. C. In *Molecular Energy Transfer in Gases*; Butterworth Scientific: London, 1961.
(6) Keeton, R. G.; Bass, H. E. *J. Acoust. Soc. Am.* **1976**, *60*, 78.
(7) Yardley, J. T. *Introduction to Molecular Energy Transfer*; Academic: New York, 1980.
(8) Heymann, M.; Hippler, H.; Plach, H. J.; Troe, J. *J. Chem. Phys.* **1987**, *87*, 3867.
(9) Hippler, H.; Otto, B.; Troe, J. *Ber. Bunsen-Ges. Phys. Chem.* **1989**, *93*, 428.
(10) Hippler, H.; Troe, J. In *Bimolecular Collisions*; Ashfold, M. N. R., Baggott, J. E., Eds.; Royal Society of Chemistry: London, 1989.
(11) Barker, J. R.; Toselli, B. M. *Int. Rev. Phys. Chem.* **1993**, *12*, 305.
(12) Rossi, M. J.; Pladziewicz, J. R.; Barker, J. R. *J. Chem. Phys.* **1983**, *78*, 6695.
(13) Yerram, M. L.; Brenner, J. D.; King, K. D.; Barker, J. R. *J. Phys. Chem.* **1990**, *94*, 6341.
(14) Toselli, B. M.; Walunas, T. L.; Barker, J. R. *J. Chem. Phys.* **1990**, *92*, 4793.
(15) McDowell, D. R.; Wu, F.; Weisman, B. *J. Chem. Phys.* **1988**, *108*, 9404.
(16) Zheng, L.; Chou, J.; Flynn, G. W. *J. Phys. Chem.* **1991**, *95*, 6759.
(17) Mullin, A. S.; Park, J.; Chou, J. Z.; Flynn, G. W.; Weston, R. E. *J. Chem. Phys.* **1993**, *175*, 53.
(18) Mullin, A. S.; Michaels, C. A.; Flynn, G. W. *J. Chem. Phys.* **1995**, *102*, 6032.
(19) Michaels, C. A.; Mullin, A. S.; Flynn, G. W. *J. Chem. Phys.* **1995**, *102*, 6682.
(20) Michaels, C. A.; Lin, Z.; Mullin, A. S.; Flynn, G. W. *J. Chem. Phys.* **1997**, *106*, 7055.
(21) Michaels, C. A.; Mullin, A. S.; Park, J.; Chou, J.; Flynn, G. W. *J. Chem. Phys.* **1998**, *108*, 2744.
(22) Wall, M. C.; Stewart, B. A.; Mullin, A. S. *J. Chem. Phys.* **1998**, *108*, 6185.
(23) Wall, M. C.; Mullin, A. S. *J. Chem. Phys.* **1998**, *108*, 9658.
(24) Wall, M. C.; Lemoff, A. S.; Mullin, A. S. *J. Phys. Chem.* in press.
(25) Elioff, M. S.; Wall, M. C.; Lemoff, A. S.; Mullin, A. S. *J. Chem. Phys.* manuscript in preparation.
(26) Dietz, T. G.; Duncan, M. A.; Pulu, A. C.; Smalley, R. E. *J. Phys. Chem.* **1982**, *86*, 4028.
(27) Knee, J.; Johnson, P. *J. Phys. Chem.* **1985**, *89*, 948.
(28) Nakashima, N.; Yoshihara, K. *J. Phys. Chem.* **1989**, *93*, 7763.
(29) Chesko, J. D.; Stranges, D.; Suits, A. G.; Lee, Y. T. *J. Chem. Phys.* **1995**, *103*, 6290.
(30) Michaels, C. A.; Tapalian, H. C.; Lin, Z.; Sevy, E. T.; Flynn, G. W. *Faraday Discuss.* **1995**, *102*, 405.
(31) Nelson, D. D.; Schiffman, A.; Lykke, K. R.; Nesbitt, D. J. *Chem. Phys. Lett.* **1988**, *153*, 105.
(32) *HITRAN Spectral Database*; Air Force Research Labs, Phillips Labs, 1996.
(33) Herzberg, G. *Molecular Spectra and Molecular Structure II: Infrared and Raman Spectra*; Van Nostrand Reinhold: New York, 1945.
(34) Miller, L. A.; Barker, J. R. *J. Chem. Phys.* **1996**, *105*, 1383.
(35) Toselli, B. M.; Barker, J. R. *J. Chem. Phys.* **1992**, *97*, 1809.